Catalysis Science & Technology

Accepted Manuscript

This is an *Accepted Manuscript*, which has been through the Royal Society of Chemistry peer review process and has been accepted for publication.

Accepted Manuscripts are published online shortly after acceptance, before technical editing, formatting and proof reading. Using this free service, authors can make their results available to the community, in citable form, before we publish the edited article. We will replace this *Accepted Manuscript* with the edited and formatted *Advance Article* as soon as it is available.

You can find more information about *Accepted Manuscripts* in the Information for Authors.

Please note that technical editing may introduce minor changes to the text and/or graphics, which may alter content. The journal's standard Terms & Conditions and the Ethical guidelines still apply. In no event shall the Royal Society of Chemistry be held responsible for any errors or omissions in this *Accepted Manuscript* or any consequences arising from the use of any information it contains.

ROYAL SOCIETY OF CHEMISTRY

www.rsc.org/catalysis

Journal Name

ARTICLE

Reversible cyclometalation at Rh^I as Motif for Metal-Ligand Bifunctional Bond Activation and Base-free Formic Acid Dehydrogenation

Received 00th January 20xx,
Accepted 00th January 20xx

DOI: 10.1039/x0xx00000x

www.rsc.org/

L. S. Jongbloed,[a] B. de Bruin[a], J. N. H. Reek,[a] M. Lutz[b] and J. I. van der Vlugt[a]

Reversible cyclometalation is demonstrated as a strategy for the activation of protic small molecules, with a proof-of-principle catalytic application in the dehydrogenation of formic acid, in the absence of exogenous base. The well-defined Rh^I complex Rh(CO)(**L**) **1**, bearing the reactive cyclometalated PN(C) ligand **L** (**L**^{H} = PNC^H = 2-di(*tert*-butylphosphinomethyl)-6-phenylpyridine) undergoes protonolysis of the Rh-C_{Ph} bond with weak protic reagents, such as thiols and trifluoromethanesulfonamide. This system als displays bifunctional metal-ligand protonolysis reactivity with formic acid and subsequent decarboxylation of the formate complex. DFT calculations show that H_2 evolution from a putative Rh(CO)(H)(**L**^{H}) complex **A** is very facile, encompassing formal C-H oxidative addition at Rh to give **C** via agostic intermediate **B** and subsequent reductive elimination of H_2. Complex **1** is a catalytically competent species for base-free formic acid dehydrogenation, involving formate intermediate **4**. Density functional theory (DFT) calculations reveal accessible barriers for involvement of the flanking phenyl group for both initial activation of the formic acid and release of H_2, supporting a cooperative pathway. Reversible C-H activation is thus a viable mechanism for metal-ligand bifunctional catalysis.

Introduction

The application of reactive ligands for metal-ligand bifunctional bond activation and subsequent cooperative catalysis receives much attention.[1] Among the different reactive ligand designs, systems bearing a proton-responsive group (showing reversible deprotonation activity) are particularly attractive and versatile. Generally, two strategies to incorporate such a fragment (an 'internal base') within the ligand structure that can easily activate substrates co-exist: i) a site in the coordination sphere of a metal center and ii) a site at a location not directly connected to the metal center (2nd coordination sphere). Well-known designs implementing the latter strategy operate via reversible dearomatization by deprotonation of functionalized picoline,[2] aminopyridine,[3] or pyridone fragments.[4] Regarding the strategy encompassing proton-responsive groups in the coordination sphere of a transition metal, reversible deprotonation of metal-bound functionalized amines[5] has been successfully applied in a variety of catalytic transformations.

Metal-carbon bonds are typically rather strong, but the bond energy can be influenced by e.g. strain or non-ideal orbital overlap, as present in cyclometalated species. Reversible cyclometalation at late transition metals using strong acids has been well-documented for stoichiometric scenarios,[6,7,8] but examples with low-valent metal ions such as Rh^I and applications of this type of reactivity in catalytic turnover are rare, to the best of our knowledge. Metal-ligand bifunctional catalysis by reversible cyclometalation has been postulated as possible mechanism with a few systems (Figure 1). Mashima *et al.* discussed this strategy for the dehydrogenative silylation of phenylpyridines catalyzed by a cyclometalated iridium complex.[9] A similar 'roll-over' mechanism was suggested for the base-free transfer hydrogenation with a ruthenium catalyst.[10] The cooperativity of a cyclometalated fragment in the ligand structure has also been proposed, on the basis of computational studies, to be suitable for the dehydrogenation of ammonia-borane.[11,12,13] However, it was experimentally proven that this mechanism occurs most likely only in the early stage of catalysis[13] or as a way to generate an active species.[12]

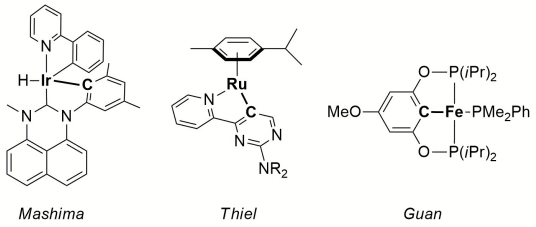

Figure 1. Complexes that have been proposed to act as cooperative catalysts for different types of transfomations via reversible cyclometalation.

Computational studies by Vanka *et al.* indicate that reversible cyclometalation can not only be useful for NH_3BH_3

[a] *Homogeneous, Bioinspired & Supramolecular Catalysis, van 't Hoff Institute for Molecular Sciences, University of Amsterdam, Science Park 904, 1098 XH Amsterdam, the Netherlands. E-mail: j.i.vandervlugt@uva.nl*
[b] *Crystal & Structural Chemistry, Bijvoet Center for Biomolecular Research, Utrecht University, Padualaan 8, 3584 CH, the Netherlands*

Electronic Supplementary Information (ESI) available: spectroscopic, crystallographic, catalytic and computational details. See DOI: 10.1039/x0xx00000x

Catalysis Science & Technology Accepted Manuscript

dehydrogenation but also be a suitable mechanism for formic acid dehydrogenation to CO_2 and H_2.[11] Dihydrogen is a considered a key component of many future renewable energy solutions, but efficient and reversible storage and release of H_2, e.g. in organic liquids such as formic acid (FA), is essential for a hydrogen based economy. Most catalytic systems for the dehydrogenation of HCOOH to H_2 and CO_2 require the presence of exogenous base,[14] which not only decreases the overall hydrogen content from 4.4 wt% (for pure HCOOH) to 2.3 wt% (for a typical 5:2 HCOOH/NEt_3 mixture) but also necessitates post-catalysis processing for fuel cell applications (removal of volatile amines).[15] Hence, catalytic formic acid dehydrogenation should ideally be performed in the absence of such exogenous base, but to date only a handful of systems capable of base-free formic acid dehydrogenation have been reported.[16]

Given our interest in the design of reactive ligand systems for cooperative bond activation reactions and catalytic processes,[17] we wondered whether reversible C-H activation in the coordination sphere of a metal could serve as a new methodology to facilitate e.g. formic acid dehydrogenation. In such a strategy, a metal-carbon fragment should function as an internal base for the activation of a suitable protic substrate. A hypothetical cooperative mechanism based on reversible cyclometalation as a bond-activation concept involves i) M-C bond assisted E-H bond activation and ii) ligand-assisted Y-H bond reductive elimination after productive conversion of the activated M-E moiety into a product-like M-Y fragment (Scheme 1). Reversible cyclometalation by protonation of the M-C bond might result in a weakly coordinating agostic C-H bond.[18] This fragment could be viewed as masking a vacant site at the metal center, without significant pertubations (structural or electronic) of the global ligand framework, unlike what is often encountered for other reactive ligands. An agostic C-H interaction might also assist in stabilizing catalytically relevant intermediates, with beneficial implications for the overall energy profile of a potential reaction path.

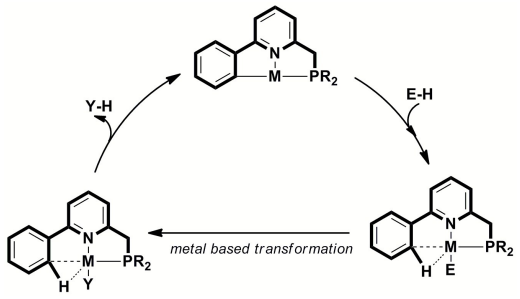

Scheme 1. Proposed pathway involving reversible cyclometalation for metal-ligand bifunctional bond activation and catalysis.

Recently, we synthesized cyclometalated Rh^I complex **1**[19] bearing the deprotonated derivative of ligand $\mathbf{L^H}$ that can act both as a neutral bidentate PN-ligand and as anionic tridentate PNC-system, depending on the reaction conditions. Based on these initial results, we speculated that the ligand-based reactive carbon center in the coordination sphere of Rh^I could be employed as internal base for the activation and conversion of functionalized protic substrates and the flexidentate character of the ligand could be beneficial in catalysis. We previously studied the activation of alkynes,[20] activated amines[21] and thiols[22,23] using proton-responsive PN and PNP ligands coordinated to late transition metals using dearomatization/aromatization cooperativity. In this article we describe the reactivity of the Rh-C bond toward related substrates and we report on the base-free dehydrogenation of formic acid as proof-of-principle for the use of reversible cyclometalation in metal-ligand bifunctional catalysis.

Results and discussion

Reactivity of 1 toward weak protic donors - thiols. The cyclometalated complex **1** was shown to be susceptible to Rh-C cleavage by ethereal HBF_4 as strong acid. This generates a Rh^I complex with an agostic Rh-(C_{Ph}-H) bond in the solid state, possibly via protonation of the metal to create a Rh^{III}(hydride) intermediate, with subsequent C-H reductive elimination. Furthermore, facile methylation at the cyclometalated carbon results from reaction of **1** with MeI. Based on these initial results, the activation of less reactive substrates was investigated. Initial attempts to activate alcohols or phenylacetylene at r.t. did not result in Rh-C cleavage, based on NMR spectroscopy. This may point toward either a pK_a mismatch between these protic substrates and the metal-carbon bond as 'internal base' or to unfavorable steric interference that prevents formal oxidative addition at the metal center.

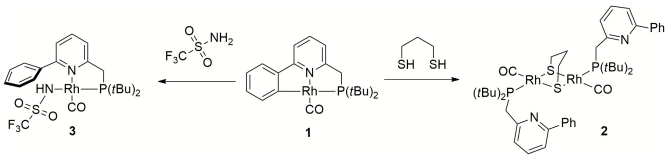

Scheme 2. Reactivity of Rh^I complex **1** toward 1,3-propanedithiol and trifluoromethanesulfonamide.

Aliphatic thiols did react smoothly with **1**, judging from the rapid color change of the solution from red to light-yellow (Scheme 2). ^{31}P NMR spectroscopy proved very useful to monitor the chemistry at the Rh-C bond *trans* to the phosphine donor. Hence, while **1** appears as a doublet at δ 76.31 ppm ($^1J_{Rh-P}$ = 101 Hz), the reaction with 1,3-propanedithiol led to a doublet at δ 69.75 ppm ($^1J_{Rh-P}$ = 151.7 Hz) for complex **2**. A strong IR-band for the carbonyl was present at ν 1938 cm^{-1} (Δν of 5 cm^1 *vs* **1**), while the pyridine signals were significantly shifted downfield in the ^1H NMR spectrum. These data suggest decoordination of the pyridine donor and thus monodentate P-coordination of the PNC^H framework, induced by the tendency of thiolate fragments to bridge to metal centers. This hypothesis was corroborated by X-ray crystal structure determination on single crystals of **2** grown from a concentrated acetone-d_6 solution (Figure 2). The geometry around each Rh^I-center is square planar and the

Catalysis Science & Technology Accepted Manuscript

This journal is © The Royal Society of Chemistry 20xx

Please do not adjust margins

overall structural features with the *gem*-dithiolate core resemble those reported in literature.[24]

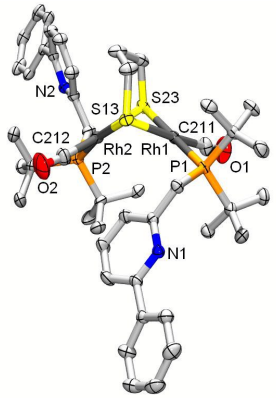

Figure 2. ORTEP plot (50% displacement ellipsoids) for complex **2**. Selected bond lengths (Å) and angles (°): Rh_1-P_1 2.3163(5); Rh_1-C_{211} 1.827(2); Rh_1-S_{13} 2.3940(5); Rh_1-S_{23} 2.3784(5); Rh_2-P_2 2.3154(6); Rh_1-C_{212} 1.808(2); Rh_2-S_{13} 2.3833(5); Rh_2-S_{23} 2.3948(5); Rh_1…Rh_2 3.0845(2); P_1-Rh_1-S_{13} 94.682(18); S_{13}-Rh_1-S_{23} 82.762(18); P_2-Rh_2-S_{23} 93.690(19); S_{13}-Rh_2-S_{23} 82.642(18). Angle sums Rh_1: 359.99(10); Rh_2: 360.44(12) °. Dihedral angle between S-Rh-S planes: 61.27(3)°.

Similar spectroscopic observations were made when reacting **1** with benzyl mercaptan.[25] This behaviour is strikingly different from the chemistry observed for Ni-complexes with dearomatized PNP ligands, by virtue of the tridentate ligand coordination,[22] although for Cu^{I}, this PNP scaffold was shown to adopt a dinucleating coordination mode.[23] Because of the decoordination of the pyridine from the metal, we did not pursue catalytic (hydroaddition) transformations involving thiols, as the proposed cooperative nature of reversible cyclometalation is aided by close proximity of the C-H bond to the metal by the directing force of the pyridine group. Also trifluoromethylsulfonamide reacts rapidly with the Rh-C bond (Scheme 2), which resulted in a ^{31}P shift for the resulting amide complex **3** at δ 103.7 ppm ($^{1}J_{RhP}$ = 152 Hz). The combined spectroscopic data are similar to previously reported $Pd(CH_3)(^{R}PN)$(triflamide) species,[21] so a similar geometry, with the triflamide *trans* to phosphorus, is proposed, although single crystalline material could not be obtained for this compound.

DFT calculations on H_2 activation with 1. Having demonstrated that cyclometalated Rh^{I}-system **1** is reactive toward (weakly) protic substrates, we sought to apply the concept of reversible cyclometalation in cooperative catalysis. Species **1** appeared stable under an H_2 atmosphere (20 bar) at r.t., indicating a relatively high barrier for heterolytic cleavage of H_2, which would generate putative species **A**, Rh(H)(CO)(**1**^{H}). Heating an NMR sample for 1 hour at 70 °C under 35 bar of H_2 did not result in any observable hydride species. This 'inertness' toward heterolytic H_2 activation can be taken as indication that the reverse reaction, i.e. H_2 evolution from **C** to generate **1**, may be a favourable pathway. To confirm this hypothesis, we performed DFT calculations (BP86, def2-TVZP, disp3 corrections) on monohydride complex **A** (Figure 3). This species may convert, via agostic intermediate **B** and subsequent C_{Ph}-H oxidative addition, to dihydride **C** with a low barrier 7.2 kcal mol^{-1}. This dihydride subsequently undergoes smooth reductive elimination of H_2 (6.9 kcal mol^{-1} barrier) to generate **1** as stable product (ΔG = -7.6 kcal mol^{-1}). As a result, this cyclometalated complex may thus be a catalytically competent species for reactions that involve H_2 production.

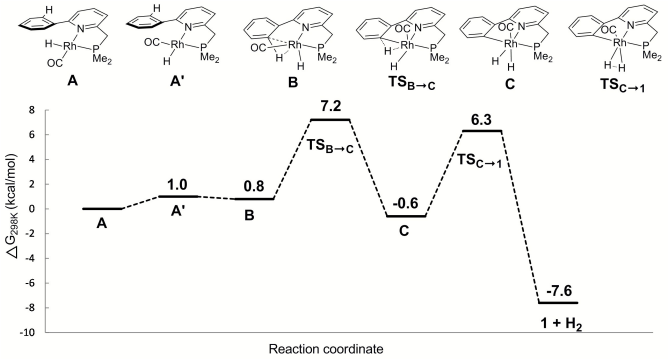

Figure 3. DFT (BP86, def2-TZVP, disp3) calculated free energy profile (ΔG^{0}_{298K} in kcal mol^{-1}) of hydrogen formation from hydride intermediate $\mathbf{A}^{Me}$, with methyl instead of *tert*-butyl groups.

Catalytic dehydrogenation of formic acid. To capitalize on the apparent facile loss of H_2 from putative species **A** in combination with the potential reactivity of the metal-carbon bond in a metal-ligand bifunctional dehydrogenative catalysis and to illustrate the concept of reversible metalation for cooperative bond activation, we studied the dehydrogenation of formic acid as proof-of-principle reaction. Addition of 20 molar equiv HCOOH to **1** in MeCN instantaneously resulted in a yellow complex that can be characterized as formate derivative **4** (Scheme 3). Complex **4** (^{31}P: δ 105 ppm, $^{1}J_{Rh\text{-}P}$ 167 Hz) is the only species present at r.t., but upon warming to 55 °C in a closed NMR tube, deep-red species **1** is regenerated within 45 minutes. No trace of remaining HCOOH was observed, and the formation of H_2 was detected (Figure 4).

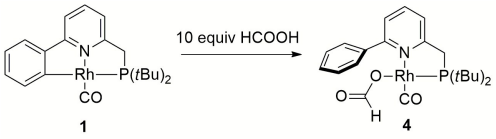

Scheme 3. Reactivity of Rh^{I} complex **1** toward 10 molar equiv of HCOOH.

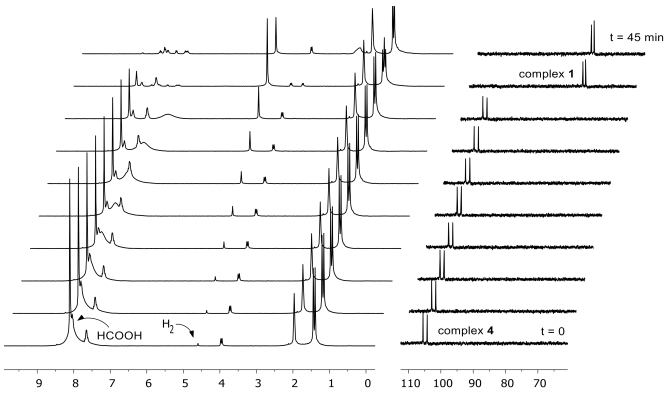

Catalysis Science & Technology Accepted Manuscript

Figure 4. Catalytic experiment (0.02 mmol cat. **1**, 0.4 mmol HCOOH, 2 mL MeCN, 55 °C → 60 °C) in 10mm HP-NMR tube, monitored by ^{1}H NMR (left) and ^{31}P NMR spectroscopy (right) over a time-span of 45 min. NMR spectra are stacked under an angle of 15°.

Use of HCOOD resulted in selective deuteration of both *ortho*-C-H groups on the phenyl ring in **1**, which is in line with cooperative activation of FA over the Rh-C bond. No deuteration of the methylene spacer was observed under these conditions, as confirmed by ^{2}H NMR studies, excluding a role for this reactive site during turnover. Smooth catalytic dehydrogenation of HCOOH was established using 0.5 mol% of species **1** in dioxane at 75 °C, with a turnover frequency (TOF) of 169 mol·mol^{-1}·h^{-1} (see Figure 5 and ESI). Addition of external base (NEt_3) did not affect the catalytic activity.[27] Catalyst **1** showed reproducible performance during eight consecutive runs (total TON of 1024). The gaseous fraction produced during reaction was analyzed by GC and no CO was found within the detection limit (δ = 10 ppm). Although the TOF achieved is still moderate under these (unoptimized) conditions, this represents the first example of base-free formic acid dehydrogenation using a Rh^{I} complex.[27]

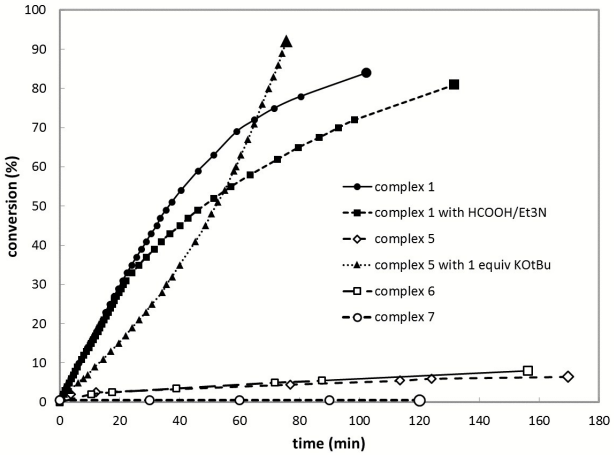

Figure 5. Catalytic dehydrogenation curves.

Control experiments using complex **5** ([Rh(Cl)(CO)(PN^{H}])) bearing a bidentate PN^{H} ligand (Figure 6),[20,21] lacking the flanking phenyl arm, showed very low conversion in absence of base, likely due to blocking of the fourth coordination site by the chloride ligand. Upon addition of one equivalent of strong base to deprotonate the PN^{H} ligand, the system showed a similar TOF but a different reaction profile including significant substrate inhibition, suggesting a different catalytic pathway for this catalyst compared to complex **1** (Figure 4). This species likely follows a pathway involving ligand 'dearomatization'. The known Rh^{I}-pincer complexes [Rh(CO)(PNN*)][28] (**6**) and [Rh(CO)(PCP)][29] (**7**) (PNN* = 6-di(*tert*-butyl)phosphinomethine-2,2'-bipyridine; see Figure 5) barely gave activity, suggesting that low-coordinate geometries and the presence of a ligand with adaptable denticity are important.

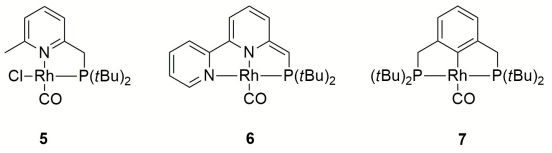

Figure 6. Other Rh^{I} complexes that were studied in the dehydrogenation of formic acid.

Mechanistic considerations. Based on these catalytic results and supported by DFT calculations, two catalytic cycles are conceivable (Scheme 4). The first intramolecular path involves reversible cyclometalation as key element. Cooperative activation of formic acid over the reactive Rh-C fragment to form formate species **4** proceeds with a moderate barrier of 17.4 kcal mol^{-1}. The transition state for a concerted hydride-proton-transfer step[30] could not be found, most likely because the hydride would be located in an unfavourable axial position (filled d_z^2 orbital) at Rh. Alternatively, HCOOH could also oxidatively add to form a Rh^{III} intermediate that can undergo reductive elimination of the C_{Ph}-H bond. This option could not be ruled out by DFT calculations, as charged species cannot be compared to neutral species in gas phase calculations (see ESI). Resting state **4**, which lies -1.9 kcal mol^{-1} lower in energy than **1**, converts to monohydride **A** via rate-limiting β-H elimination (18.2 kcal mol^{-1} relative to **4**) concomitant with CO_2 release. Subsequent C-H oxidative addition via the Rh^{I}(C-H) agostic species **B** (a close analogue of a previously isolated cationic derivative[19]) and facile release of H_2 from Rh^{III} intermediate **C** regenerates **1** as the active catalyst. The reversible C-H metalation pathway, providing a hemilabile aryl moiety, is also proposed to stabilize the Rh-species between turnovers.

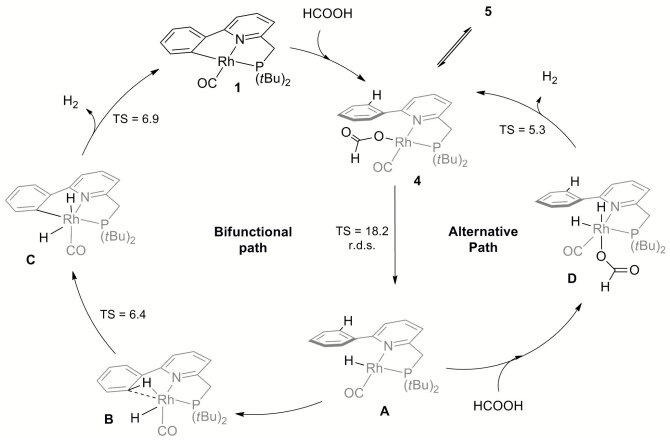

Scheme 4. Proposed mechanism for the base-free cooperative dehydrogenation of formic acid using **1** as catalyst. The DFT calculated values for the relative transition state barriers are shown in kcal mol^{-1}.

A second, non-cooperative, path has very similar reaction barriers and shares the same rate-limiting step (from **4** to **A**), followed by oxidative addition of a second molecule of HCOOH to form dihydride intermediate **D**, which lies 0.8 kcal mol^{-1} higher in energy than **A**. Dihydride **D** generates H_2 via reductive elimination with a TS barrier of 5.3 kcal mol^{-1}. Given the near-identical overall reaction profiles (with a shared rate limiting step with a barrier of ~18 kcal mol^{-1}), both mechanisms likely are catalytically competent and thus co-exist under

Catalysis Science & Technology Accepted Manuscript

This journal is © The Royal Society of Chemistry 20xx

Please do not adjust margins

catalytic conditions, regenerating red species **1** during and/or after catalysis. The involvement of the cooperative path is supported by selective deuteration experiments, isolation of an agostic C-H model complex as a relevant intermediate,[19] the spectroscopic observation of **4** in the presence of 10 equivalents of formic acid, followed by regeneration of **1** with conversion of HCOOH and release of H_2.

Conclusions

In summary, we have shown that reversible cyclometalation may be successfully employed as motif for cooperative bond activation processes. Complex **1** readily reacts with thiols and activated amines, which leads to protonation of the anionic carbon of the reactive flexidentate[31] ligand **L**. DFT calculations show that release of dihydrogen is facile from a putative monohydride complex **A**. Reaction of cyclometalated complex **1** with a small excess of formic acid results in formate adduct **4**. To demonstrate the potential of reversible cyclometalation in metal-ligand bifunctional catalysis, we have successfully employed Rh^{I} catalyst **1** in the base-free dehydrogenation of formic acid. Experimental observations in combination with DFT studies support a cooperative mode of action based on reversible cyclometalation as a feasible mechanism.

Experimental

General considerations

All reactions were carried out under an atmosphere of nitrogen using standard Schlenk techniques. Reagents were purchased from commercial suppliers and used without further purification. THF, pentane, hexane and Et_2O were distilled from sodium benzophenone ketyl. CH_2Cl_2 was distilled from CaH_2, toluene from sodium under nitrogen. NMR spectra (^{1}H, ^{1}H{^{31}P}, ^{31}P, ^{31}P{^{1}H}, ^{31}P-^{1}H and ^{13}C{^{1}H}) were measured on a Bruker DRX 500, Bruker AV 400, Bruker DRX 300 or on a Bruker AV 300 spectrometer. IR spectra (ATR mode) were recorded with a Bruker Alpha-p FT-IR spectrometer. High resolution mass spectra were recorded on a JMS-T100GCV mass spectrometer using field desorption (FD).

Complex 2, $Rh_2(SCH_2CH_2CH_2S)(CO)_2(\kappa^1\text{-}P\text{-}1^H)_2$

To a solution of **1** (10 mg, 23 µmol) in CH_2Cl_2 (1 mL) was added 1,3-propanedithiol (1.1 µL, 23 µmol), resulting in an immediate color change from red to dark yellow. The solvent was evaporated to yield **2** in quantitative yield (11 mg). ^{1}H NMR (300 MHz, 298 K, CD_2Cl_2, ppm): δ 8.44 (d, *J* = 6.3 Hz, 2H), 8.14 – 8.07 (m, 4H), 7.63 – 7.40 (m, 10H), 4.21 – 3.82 (m, 4H), 2.95 – 2.69 (m, 4H), 2.42 – 2.30 (m, 2H), 1.53 (d, *J* = 12.7 Hz, 18H), 1.41 (d, *J* = 12.9 Hz, 18H). ^{31}P NMR (121 MHz, 298 K, CD_2Cl_2, ppm): δ 69.75 (d, *J* = 151.7 Hz). ^{13}C NMR (75 MHz, 298 K, CD_2Cl_2, ppm): δ 190.58 (dd, J_{RhC} = 73.4 Hz, J_{CP} = 14.9 Hz, CO), 157.28 (s, Py-C), 155.81 (s, Py-C), 139.48 (s, Ph-C), 136.22 (s, Py-CH), 128.71 (s, Ph-CH), 128.58 (s, 2C, Ph-CH), 126.75 (s, 2C, Ph-CH), 124.71 (d, *J* = 2.8 Hz, Py-CH), 117.89 (s, Py-CH), 38.67 (s, SCH_2CH_2), 37.31 (d, *J* = 16.2 Hz, $PC(CH_3)_3$), 36.93 (dd, *J* = 15.7, 1.3 Hz, CH_2P), 31.71 (d, *J* = 13.0 Hz, SCH_2CH_2), 30.16 (dd, *J* = 17.4, 3.8 Hz, $PC(CH_3)_3$). IR (ATR, cm^{-1}): ν_{CO} 1938. HRMS (FD): *m/z* calcd for $C_{44}H_{62}N_2OP_2Rh_2S_2$: 966.18888 $[M\text{-}CO]^+$; found: 966.18386.

Complex 3, $Rh(NHSO_2CF_3)(CO)(\kappa^2\text{-}P,N\text{-}1^H)$

To a solution of **1** (12 mg, 27 µmol) in CH_2Cl_2 (1 mL) was added trifluoromethylsulfonamide (4 mg, 27 µmol), resulting in a color change from red to orange within 5 min. at room temperature. The solvent was evaporated to yield **3** in quantitative yield (16 mg). ^{1}H NMR (300 MHz, 298 K, CD_2Cl_2, ppm): δ 8.20 – 8.12 (m, 2H, Ph), 7.90 (t, *J* = 7.8 Hz, 1H, Py), 7.68 – 7.59 (m, 3H, Ph), 7.52 (t, *J* = 8.3 Hz, 2H, Py), 3.75 (d, *J* = 9.3 Hz, 2H, CH_2P), 1.41 (d, *J* = 14.1 Hz, 18H, $PtBu_2$), 1.14 (s, 1H, NH). ^{31}P NMR (121 MHz, 298 K, CD_2Cl_2, ppm): δ 103.70 (d, *J* = 152.0 Hz). ^{19}F NMR (282 MHz, 298 K, CD_2Cl_2, ppm): δ -78.68 . ^{13}C NMR (75 MHz, 298 K, CD_2Cl_2, ppm): δ 189.59 (dd, J_{RhC} = 75.5 Hz, J_{CP} = 17.7 Hz, CO), 161.58 (s, Py-C), 161.50 (dd, *J* = 4.7, 1.8 Hz, Py-C), 139.03 (s, Py-CH and Ph-C), 130.57 (s, Ph-CH), 128.62 (s, Ph-CH), 128.52 (s, Ph-CH), 124.17 (s, Py-CH), 121.48 (d, *J* = 9.2 Hz, Py-CH), 120.88 (q, J_{CF} = 325.5 Hz, CF_3), 35.32 (dd, *J* = 20.8, 2.3 Hz, CH_2P), 34.78 (d, *J* = 20.1 Hz, $PC(CH_3)_3$), 28.92 (d, *J* = 4.2 Hz, $PC(CH_3)_3$). IR (ATR, cm^{-1}): ν_{CO} 1973 cm^{-1}. HRMS (FD): *m/z* calcd for $C_{22}H_{30}F_3N_2O_3PRhS$: 593.07219 $[M]^+$; found: 593.07219.

Complex 4, $Rh(OCH(O)(CO)(\kappa^2\text{-}P,N\text{-}1^H)$

To a solution of **1** (4.4 mg, 10 µmol) in $CDCl_3$ (0.6 mL) was added formic acid (9.2 mg, 200 µmol), resulting in an immediate color change from red to yellow at room temperature. Due to its unstable nature, this species was only characterized in situ using NMR spectroscopy. ^{1}H NMR (400 MHz, 298 K, $CDCl_3$, ppm): δ 8.01–7.94 (m, 2H, *o*-Ph), 7.82 (ddd, *J* = 7.8, 7.8, 1.0 Hz, 1H, Py), 7.57–7.39 (m, 5H, 2Py, *m*-Ph, *p*-Ph), 3.73 (d, $^2J_{P\text{-}H}$ = 9.6 Hz, 2H), 1.38 (d, $^3J_{P\text{-}H}$ = 14.3 Hz, 18H). ^{31}P NMR (162 MHz, 298 K, $CDCl_3$, ppm): δ 105.29 (d, $J_{Rh\text{-}P}$ = 166.8 Hz).

Complex 6, $Rh(Cl)(CO)(\kappa^2\text{-}P,N$-2-methyl-6-((di-tert-butylphosphino)-methyl)pyridine))

To a solution of 2-methyl-6-((di-tert-butylphosphino)methyl)-pyridine (0.025 g, 0.010 mmol) in CH_2Cl_2 (0.5 mL) was added a solution of $[Rh(CO)_2(\mu\text{-}Cl)]_2$ (0.019 g, 0.005 mmol) in CH_2Cl_2 (2 mL) and the reaction mixture was stirred overnight. After evaporation of the solvent, the product was washed with pentane (1 mL), yielding the desired complex as yellow powder (0.038 g, 0.092 mmol, 92%). ^{1}H NMR (300 MHz, 298 K, acetone-d_6, ppm): δ 7.77 (t, *J* = 7.7 Hz, 1H, Py), 7.46 (d, *J* = 7.7 Hz, 1H, Py), 7.23 (d, *J* = 7.7 Hz, 1H, Py), 3.93 (d, $^2J_{P\text{-}H}$ = 9.6 Hz, 2H, CH_2P), 3.10 (s, 3H, Py-CH_3), 1.32 (d, $^2J_{P\text{-}H}$ = 13.9 Hz, 18H, $(CH_3)CP$). ^{31}P NMR (121 MHz, 298 K, $CDCl_3$, ppm): δ 106.12 (d, $^1J_{Rh\text{-}P}$ = 165.0 Hz). ^{13}C NMR (75 MHz, 298 K, acetone-d_6, ppm): δ 191.85 (dd, *J* = 73.4, 14.5 Hz, CO), 163.78 (s, Py-C), 162.52 (d, *J* = 3.9 Hz, Py-C), 139.74 (s, Py-CH), 124.56 (Py-CH), 121.46 (d, *J* = 9.0 Hz, Py-CH), 36.05 (dd, $^1J_{C\text{-}P}$ = 20.3, $^2J_{Rh\text{-}C}$ = 2.3 Hz, CH_2P), 35.42 (d $^1J_{C\text{-}P}$ = 20.7 Hz, $PC(CH_3)_3$), 29.48 (d, $^2J_{C=P}$ = 4.5 Hz, $PC(CH_3)_3$), 28.19 (s, Py-CH_3). IR (ATR, cm^{-1}): ν_{CO} 1958. HRMS(FD): m/z calcd $C_{16}H_{26}ClNOPRh$: 417.04956 $[M]^+$; found: 417.04984.

Catalysis Science & Technology Accepted Manuscript

Catalytic dehydrogenation experiments

In a typical experiment, compound **1** (10 μmol) was added to the solvent (1 mL) in a 5 mL Schlenk equipped with a condenser and connected to a water replacement set-up. The reaction mixture was heated to the desired temperature (e.g. 75 °C) and stirred for 10 minutes. Formic acid (75 μL, 2 mmol) or the azeotrope $HCOOH/NEt_3$ (187 μL, 2 mmol HCOOH) was added to the reaction mixture and the evolved gas was collected. In the case of complex RhCl(CO)(PN), first one equivalent of potassium *tert*-butoxide in THF (1M) was added at r.t. to abstract the chloride ligand. After stirring this mixture for 5 min, 75 μL HCOOH was added. The mixture was rapidly heated to 75 °C and the evolved gas was collected. The setup was calibrated with a Brooks flowmeter type 1054-3C and evolved gases were analyzed with a G·A·S Compact GC (Rt-MSieve 5A 20 m × 0.32 mm + Rt-Q-bond 2 m × 0.32 mm).

X-ray crystal structure determination of complex 2

$C_{45}H_{62}N_2O_2P_2RhS_2$, Fw = 994.85, yellow block, 0.25 × 0.19 × 0.09 mm^3, monoclinic, $P2_1/n$ (no. 14), a = 12.7487(4), b = 19.7725(6), c = 18.4361(5) Å, β = 103.046(1) °, V = 4527.3(2) $Å^3$, Z = 4, D_x = 1.460 g/cm^3, μ = 0.93 mm^{-1}. 60826 Reflections were measured on a Bruker Kappa ApexII diffractometer with sealed tube and Triumph monochromator (λ = 0.71073 Å) at a temperature of 150(2) K up to a resolution of $(\sin\theta/\lambda)_{max}$ = 0.65 $Å^{-1}$. X-ray intensities were measured on a Bruker Kappa ApexII diffractometer with sealed tube and Triumph monochromator (λ = 0.71073 Å) at a temperature of 150(2) K. The intensities were integrated with the Eval15 software.[32] Multi-scan absorption correction and scaling was performed with SADABS[33] (correction range 0.67-0.75). 10392 Reflections were unique (R_{int} = 0.039), of which 8330 were observed [$I>2\sigma(I)$]. The structure was solved with Patterson superposition methods using SHELXT.[34] Least-squares refinement was performed with SHELXL-97[35] against F^2 of all reflections. Non-hydrogen atoms were refined freely with anisotropic displacement parameters. All hydrogen atoms were located in difference Fourier maps and refined with a riding model. 508 Parameters were refined with no restraints. R1/wR2 [$I > 2\sigma(I)$]: 0.0255 / 0.0542. R1/wR2 [all refl.]: 0.0396 / 0.0580. S = 1.023. Residual electron density between -0.32 and 0.32 e/$Å^3$. CCDC 1422009 contains the supplementary crystallographic data for this paper. These data can be obtained free of charge from The Cambridge Crystallographic Data Centre via www.ccdc.cam.ac.uk/data_request/cif.

DFT Calculations

Geometry optimizations were carried out with the Turbomole program package[36] coupled to the PQS Baker optimizer[37] via the BOpt package,[38] at the ri-DFT level using the BP86[39] functional and the resolution-of-identity (ri) method.[40] We optimized the geometries of all stationary points at the def2-TZVP basis set level,[41] using Grimme's dispersion corrections (disp3 version)[42] and a tight energy grid (m5). The identity of the transition states was confirmed by following the imaginary frequency in both directions (IRC). All minima (no imaginary frequencies) and transition states (one imaginary frequency) were characterized by calculating the Hessian matrix. ZPE and gas-phase thermal corrections (entropy and enthalpy, 298 K, 1 bar) from these analyses were calculated using standard thermodynamics.

Acknowledgements

This work was funded by the European Research Council (ERC, Starting Grant 279097, *EuReCat* to J.I.v.d.V.). We thank Sander Oldenhof for useful discussions and practical tips on FA dehydrogenation chemistry, Ed Zuidinga for MS measurements and Christophe Rebreyend and Sandra de Boer for supplying compounds **7** and **8**, respectively. The X-ray diffractometer at Utrecht University was funded by NWO.

Notes and references

1 Reviews: D. L. J. Broere, R. Plessius and J. I. van der Vlugt, *Chem. Soc. Rev.*, 2015, **44**, 6886-6915; D. Milstein, *Phil. Trans. R. Soc. A*, 2015, **373**, 20140189; O. R. Luca, R. H. Crabtree, *Chem. Soc. Rev.*, 2013, **42**, 1440-1459; J. I. van der Vlugt, *Eur. J. Inorg. Chem*., 2012, 363-375; V. Lyaskovskyy and B. de Bruin, *ACS Catal*., 2012, **2**, 270-279; T. Ikariya, *Top. Organomet. Chem*., 2011, **37**, 31-54; d) D. Milstein, *Top. Catal.*, 2010, **53**, 915-923.

2 Reviews: J. I. van der Vlugt and J. N. H. Reek, *Angew. Chem. Int. Ed*., 2009, **48**, 8832-8846; C. Gunanathan and D. Milstein, *Acc. Chem. Res.*, 2011, **44**, 588-602; C. Gunanathan and D. Milstein, *Chem. Rev.,* 2014, **114**, 12024-12087; J. R. Khusnutdinova and D. Milstein, *Angew. Chem. Int. Ed.* 2015, **54**, 12236-12273.

3 H. Li, B. Zheng, K.-W. Huang, *Coord. Chem. Rev.*, 2015, **293-294**, 116-138; B. Bichler, C. Holzhacker, B. Stöger, M. Puchberger, L. F. Veiros, K. Kirchner, *Organometallics*, 2013, **32**, 4114-4121; D. Benit-Garagorri, K. Kirchner, *Acc. Chem. Res.*, 2008, **41**, 201-213.

4 Overview: W-H. Wang, J. T. Muckerman, E. Fujita and Y. Himeda, *New J. Chem.*, 2013, **37**, 1860-1866. See also: C. M. Moore and N. K. Szymczak, *Chem. Commun*., 2013, **49**, 400-402; J. F. Hull, Y. Himeda, W.-H. Wang, B. Hashiguchi, R. Periana, D. J. Szalda, J. T. Muckerman and E. Fujita, *Nature Chem*., 2012, **4**, 383-388; R. Kawahara, K. Fujita and R. Yamaguchi, *Angew. Chem. Int. Ed.*, 2012, **51**, 12790-12794.

5 Reviews: B. Zhao, Z. Han and K. Ding, *Angew. Chem. Int. Ed.*, 2013, **52**, 4744-4788; S. Schneider, J. Meiners and B. Askevold, *Eur. J. Inorg. Chem.*, 2012, 412-429; S. Kuwata and T. Ikariya, *Dalton Trans*., 2010, **39**, 2984-2992.

6 Rh^{III}: J. R. Krumper, M. Gerisch, A. Magistrato, U. Rothlisberger, R. G. Bergman and T. D. Tilley, *J. Am. Chem. Soc.*, 2004, **126**, 12492–12502.

7 Ir^{III}: Y. Gloaguen, L. M. Jongens, M. Lutz, J. N. H. Reek, B. de Bruin and J. I. van der Vlugt, *Organometallics*, 2013, **32**, 4284–4291; F. Morandini, B. Longato and S. Bresadola, *J. Organomet. Chem.*, 1977, **132**, 291–299; J. A. Raskatov, S. Spiess, C. Gnamm, K. Brödner, F. Rominger and G. Helmchen, *Chem. Eur. J.*, 2010, **16**, 6601–6615. Pt^{II} (and Ir^{III}): S. Musa, R. Romm, C. Azerraf, S. Kozuch and D. Gelman, *Dalton Trans.*, 2011, **40**, 8760–8763. Au^{III}: D. A. Smith, D.-A. Roşca and M. Bochmann, *Organometallics*, 2012, **31**, 5998–6000. Pd^{II}: A. D. Getty and K. I. Goldberg, *Organometallics*, 2001, **20**, 2545–2551. Ru^{II}: J. Becker, T. Modl and V. H. Gessner, *Chem. Eur. J.*,

Catalysis Science & Technology Accepted Manuscript

This journal is © The Royal Society of Chemistry 20xx

Please do not adjust margins

2014, **20**, 11295–11299. Ni^{II}: D. V Gutsulyak, W. E. Piers, J. Borau-Garcia and M. Parvez, *J. Am. Chem. Soc.*, 2013, **135**, 11776–11779.

8 Roll-over complexes: L. Maidich, G. Zuri, S. Stoccoro, M. A. Cinellu, M. Masia, A. Zucca and U. Sassari, *Organometallics*, 2013, **32**, 438–448; B. Butschke and H. Schwarz, *Chem. Sci.*, 2012, **3**, 308–326; J. Kwak, Y. Ohk, Y. Jung and S. Chang, *J. Am. Chem. Soc.*, 2012, **134**, 17778–17788; A. Zucca, G. L. Petretto, M. L. Cabras, S. Stoccoro, M. A. Cinellu, M. Manassero and G. Minghetti, *J. Organomet. Chem.*, 2009, **694**, 3753–3761.

9 G. Choi, H. Tsurugi and K. Mashima, *J. Am. Chem. Soc.*, 2013, **135**, 13149-13161.

10 L. Taghizadeh Ghoochany, C. Kerner, S. Farsadpour, F. Menges, Y. Sun, G. Niedner-Schatteburg and W. R. Thiel, *Eur. J. Inorg. Chem.*, 2013, 4305–4317.

11 K. Ghatak, M. Mane and K. Vanka, *ACS Catal.*, 2013, **3**, 920-927.

12 C. Boulho and J.-P. Djukic, *Dalton Trans.*, 2010, **39**, 8883-8905.

13 P. Bhattacharya, J. A. Krause and H. Guan, *J. Am. Chem. Soc.*, 2014, **136**, 11153-11161.

14 Selected recent examples: R. Tanaka, M. Yamashita, L. W. Chung, K. Morokuma, K. Nozaki, *Organometallics* 2011, **30**, 6742–6750; E. A. Bielinski, P. O. Lagaditis, Y. Zhang, B. Q. Mercado, C. Würtele, W. H. Bernskoetter, N. Hazari and S. Schneider, *J. Am. Chem. Soc.*, 2014, **136**, 10234-10237; G. A. Filonenko, R. van Putten, E. N. Schulpen, E. J. M. Hensen and E. A. Pidko, *ChemCatChem*, 2014, **6**, 1526-1530.

15 B. Loges, A. Boddien, H. Junge, M. Beller, *Angew. Chem. Int. Ed.*, 2008, **47**, 3962–3965; S. Enthaler, J. von Langermann and T. Schmidt, *Energy Environ. Sci.*, 2010, **3**, 1207–1217; A. Boddien, C. Federsel, P. Sponholz, D. Mellmann, R. Jackstell, H. Junge, G. Laurenczy, M. Beller, *Energy Environ. Sci.,* 2012, **5**, 8907-8911.

16 Y. Gao, J. Kuncheria, R. J. Puddephatt and G. P. A. Yap, *Chem. Commun*., 1998, 2365-2366; A. Boddien, D. Mellmann, F. Gärtner, R. Jackstell, H. Junge, P. J. Dyson, G. Laurenczy, R. Ludwig and M. Beller, *Science*, 2011, **333**, 1733-1736; J. F. Hull, Y. Himeda, W.-H. Wang, B. Hashiguchi, R. Periana, D. J. Szalda, J. T. Muckerman and E. Fujita, *Nature Chem.*, 2012, **4**, 383-388; J. H. Barnard, C. Wang, N. G. Berry and J. Xiao, *Chem. Sci.*, 2013, **4**, 1234-1244; R. E. Rodríguez-Lugo, M. Trincado, M. Vogt, F. Tewes, G. Santiso-Quinones and H. Grützmacher, *Nature Chem.*, 2013, **5**, 342-347; S. Oldenhof, B. de Bruin, M. Lutz, M. A. Siegler, F. W. Patureau, J. I. van der Vlugt and J. N. H. Reek, *Chem. Eur. J.*, 2013, **19**, 11507-11511; W.-H. Wang, S. Xu, Y. Manaka, Y. Suna, H. Kambayashi, J. T. Muckerman, E. Fujita and Y. Himeda, *ChemSusChem*, 2014, **7**, 1976–1983; T. W. Myers and L. A. Berben, *Chem. Sci*., 2014, **5**, 2771-2777; F. Bertini, I. Mellone, A. Ienco, M. Peruzzine and L. Gonsalvi, *ACS Catal.*, 2015, **5**, 1254-1265; J. Kethandaraman, M. Czaun, A. Goeppert, R. Haiges, J. P. Jones, R. B. May, G. K. S. Prakash and G. A. Olah *ChemSusChem*, 2015, **8**, 1442-1451.

17 J. I. van der Vlugt, E. A. Pidko, D. Vogt, M. Lutz and A. L. Spek, *Inorg. Chem*., 2009, **48**, 7513-7515; J. I. van der Vlugt, M. Lutz, E. A. Pidko, D. Vogt and A. L. Spek, *Dalton Trans*., 2009, 1016-1023; J. I. van der Vlugt, M. A. Siegler, M. Janssen, D. Vogt and A. L. Spek, *Organometallics*, 2009, **28**, 7025-7032; R. C. Bauer, Y. Gloaguen, M. Lutz, J. N. H. Reek, B. de Bruin and J. I. van der Vlugt, *Dalton Trans*., 2011, **40**, 8822-8829; Y. Gloaguen, W. Jacobs, B. de Bruin, M. Lutz and J. I. van der Vlugt, *Inorg. Chem*., 2013, **52**, 1682-1684; V. Vreeken, M. A. Siegler, B. de Bruin, J. N. H. Reek, M. Lutz and J. I. van der Vlugt, *Angew. Chem. Int. Ed.*, 2015, **54**, 7055-7059; ; Z. Tang, E. Otten, J. N. H. Reek, J. I. van der Vlugt and B. de Bruin, *Chem. Eur. J.*, 2015, **21**, 12683-12693; S. Oldenhof, M. Lutz, J. I. van der Vlugt and J. N. H. Reek, *Chem. Commun*., 2015, **51**, 15200-15203.

18 M. Brookhart, M. L. H. Green, *J. Organomet. Chem.*, 1983, **250**, 395-408; M. Brookhart, M. L. H. Green, G. Parkin, *Proc. Natl. Acad. Sci. USA*, 2007, **104**, 6908-6914.8

19 L. S. Jongbloed, B. de Bruin, J. N. H. Reek, M. Lutz and J. I. van der Vlugt, *Chem. Eur. J.*, 2015, **21**, 7297-7305.

20 S. Y. de Boer, Y. Gloaguen, M. Lutz and J. I. van der Vlugt, *Inorg. Chim. Acta*, 2012, **380**, 336-342.

21 S. Y. de Boer, Y. Gloaguen, J. N. H. Reek, M. Lutz and J. I. van der Vlugt, *Dalton Trans.*, 2012, **41**, 11276–11283;

22 J. I. van der Vlugt, M. Lutz, E. A. Pidko, D. Vogt and A. L. Spek, *Dalton Trans.*, 2009, 1016–1023.

23 J. I. van der Vlugt, E. A. Pidko, R. C. Bauer, Y. Gloaguen, M. K. Rong and M. Lutz, *Chem. Eur. J.*, 2011, **17**, 3850–3854.

24 M. A. F. Hernandez-Gruel, G. Gracia-Arruego, A. B. Rivas, I. T. Dobrinovitch, F. J. Lahoz, A. J. Pardey, L. A. Oro and J. J. Pérez-Torrente, *Eur. J. Inorg. Chem.*, 2007, 5677–5683; F. Monteil, R, Queau and P. Kalck, *J. Organomet. Chem.,* 1994, **480**, 177-184; W. D. Jones, J. Garcia and H. Torrens, *Acta Cryst. E*, 2005, **61**, m2204-m2206.

25 Notably, reaction of **1** with thiophenol gave different spectral features, with a doublet at 99 ppm ($^1J_{Rh\text{-}P}$ = 136.3 Hz) in MeCN-d_3. When C_6D_6 was used as solvent, two species with similar shifts and coupling constants as complex **2** were observed, i.e. doublets at 66 ppm ($^1J_{Rh\text{-}P}$ = 152.1 Hz) and 72 ppm ($^1J_{Rh\text{-}P}$ = 152.9 Hz). The species interconvert when the solvent is changed in the same sample. These results indicate that monomeric complexes are formed when polar solvents are used in the reaction, but no conclusive evidence could be obtained.

26 The catalytic dehydrogenation of formic acid is not faster when the azeotrope $HCOOH/Et_3N$ 5:2 is used, but the TOF can be increased as more equivalents of the azeotrope are added under the same conditions. Increasing the formic acid concentration without a base present results in a loss of activity, presumably because dormant species **5** is formed at too high concentrations of acid.

27 Formate decomposition: E. N. Yurchenko and N. P. Anikeenko, *React. Kinet. Catal. Lett*., 1975, **2**, 65-72. CO_2 hydrogenation: J.-C. Tsai and K. M. Nicholas, *J. Am. Chem. Soc*. 1992, **114**, 5117-5124.

28 Y. Gloaguen, C. Rebreyend, M. Lutz, P. Kumar, M. I. Huber, J. I. van der Vlugt, S. Schneider and B. de Bruin, *Angew. Chem. Int. Ed.*, 2014, **53**, 6814-6818.

29 K.-W. Huang, D. C. Grills, J. H. Han, D. J. Szalda and E. Fujita, *Inorg. Chim. Acta*, 2008, **361**, 3327-3331.

30 S. Oldenhof, M. Lutz, B. de Bruin, J. I. van der Vlugt and J. N. H. Reek, *Chem. Sci.*, 2015, **6**, 1027-1034. See also: S. Oldenhof, J. I. van der Vlugt and J. N. H. Reek, *Catal. Sci. Technol.*, 2015, doi: 10.1039/C5CY01476J.

31 R. Lindner, B. van den Bosch, M. Lutz, J. N. H. Reek and J. I. van der Vlugt, *Organometallics*, 2011, **30**, 499-510.

32 A. M. M. Schreurs, X. Xian, L. M. J. Kroon-Batenburg, *J. Appl. Cryst.* 2010, **43**, 70–82.

33 G. M. Sheldrick, *SADABS*, Universität Göttingen, Germany, 2008.

34 G. M. Sheldrick, *Acta Cryst. A*, 2015, **71**, 1-8.

35 G. M. Sheldrick, *Acta Cryst. A*, 2008, **64**, 112–122.

36 R. Ahlrichs, *Turbomole Version 6.5*, Theoretical Chemistry Group, University of Karlsruhe, 2013.

37 Parallel Quantum Solutions, *PQS version 2.4,* Fayetteville, Arkansas (USA), 2001. The Baker optimizer is available separately from PQS upon request: I. Baker, *J. Comput. Chem*. 1986, **7**, 385–395.

38 P. H. M. Budzelaar, *J. Comput. Chem*., 2007, **28**, 2226–2236.

39 A. D. Becke, *Phys. Rev. A*, 1988, **38**, 3098–3100; J. P. Perdew, *Phys. Rev. B*, 1986, **33**, 8822–8824.

Catalysis Science & Technology Accepted Manuscript

40 M. Sierka, A. Hogekamp, R. Ahlrichs, *J. Chem. Phys.*, 2003, **118**, 9136–9148.
41 A. Schäfer, H. Horn, R. Ahlrichs, *J. Chem. Phys.*, 1992, **97**, 2571–2577.
42 S. Grimme, J. Antony, S. Ehrlich, H. Krieg, *J. Chem. Phys.*, 2010, **132**, 154104–154119.

Catalysis Science & Technology Accepted Manuscript

This journal is © The Royal Society of Chemistry 20xx

Please do not adjust margins

The first example of base-free catalytic dehydrogenation of formic acid using reversible cylcometalation at Rh(I) is discussed, using a combination of experimental and computational methods.

Graphical Abstract

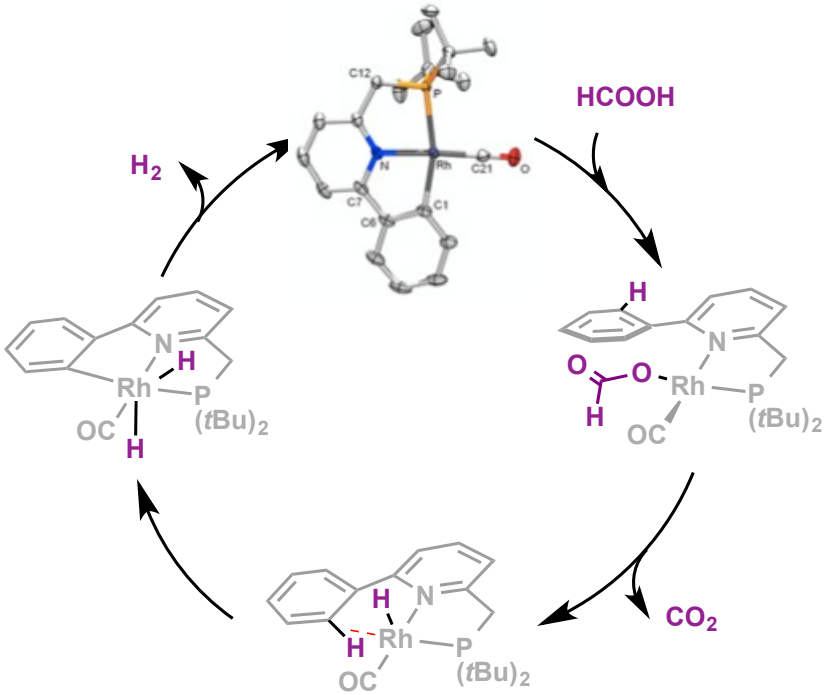

Catalysis Science & Technology Accepted Manuscript